Automated Drug Infusion System Based on Deep Convolutional Neural Networks

Koji Kashihara
Graduate School of Technology, Industrial and Social Sciences
Tokushima University
2-1 Minamijyousanjima, Tokushima, Japan
kojikasi@is.tokushima-u.ac.jp

***Abstract*—Emergent medical treatment with a vasopressor agent is needed for acute and severe hypotension during surgery. However, especially in areas with a physician shortage, busy physicians and/or anesthesiologists must control hemodynamics by using therapeutic agents. Under such conditions, an automated control system would be useful for regulating hemodynamics such as arterial pressure (AP) and cardiac output. This study designed and evaluated an adaptive predictive controller based on deep convolutional neural networks (DCNN). Compared with a standard neural networks (SNN) controller, the DCNN controller was able to stably regulate AP response to norepinephrine (NE) as a vasopressor agent and hold the desired value even under an unknown AP response. The DCNN controller could facilitate the development of an automated drug infusion system, providing a robust and simple extensibility.**

Keywords—automated control system; arterial blood pressure; catecholamines; artificial intelligence.

I. Introduction

A vasopressor agent (e.g., catecholamines) makes it possible to quickly recover mean arterial pressure (AP) from acute hypotension [1],[2]. However, the nonlinear dynamic response to a therapeutic agent complicates AP regulation. Anesthesiologists and clinicians who are busy with the patient's other clinical needs must also control the patient's hemodynamic responses to drugs [3]. Moreover, it may be difficult for inexperienced staff or interns to appropriately regulate a sudden change in hemodynamics. Therefore, developing an automated drug infusion system could positively affect a patient's treatment during or after emergent surgery as well as prove useful in local areas suffering from physician shortages.

At the initial stage in the development of automated drug infusion systems, proportional-integral-derivative (PID) controllers have been assessed in AP regulation cases [4],[5]. However, PID controllers may not make a significant contribution under the nonlinear and time-varying AP response [6],[7]. In contrast, adaptive controllers are able to adjust their parameters to optimal values, reflecting the time-varying features of AP responses [8],[9]. Traditional adaptive controllers, however, may not be able to handle nonlinear dynamics during severe or acute hypotension.

Artificial neural networks (ANN) can learn and identify nonlinear time-varying systems of a patient's vital signs. In fact, an adaptive predictive controller based on ANN has been more robust, compared to conventional controllers [10],[11]. Furthermore, deep convolutional neural networks (DCNN) have recently shown the ability to accurately abstract image features and classify image categories [12]. DCNN could also become a more efficient tool than standard neural networks (SNN) for nonlinear dynamic system identification because of analyzing measured time-course data as image features. However, the optimal technique for a DCNN controller has not been established. The purpose of this study was to construct a method for a DCNN-based AP control. The DCNN control performance was evaluated in comparison with SNN control performance. DCNN could be applied to an adaptive predictive controller to forecast future responses by mimicking a nonlinear dynamic system.

II. Control Methods

A. Modeling of Drug Response

Mathematical modeling of AP response to an infusion of norepinephrine (NE) as a vasopressor agent was created from previous data [10]. The average step response (n = 3 in rabbits) was acquired as AP changed from baseline during a 5-min infusion of NE (infusion rate of 3 μg/kg/min). AP response (sampling rate of 10 Hz) was averaged every 10 s. The AP response was calculated by the convolution integral in the discrete-time domain:

$$\begin{cases} \Delta AP^*(t) = \sum_{\tau=0}^{m} I(\tau)u(t-\tau)\,\Delta T & (1) \\ I(\tau) = \frac{K_u}{T_c} exp\left(-\frac{\tau - L}{T_c}\right), & (2) \end{cases}$$

where $u(.)$ is the infusion rate of NE (μg/kg/min); $I(.)$ is the unit impulse response computed from the derivative values of a step response (mmHg); ΔT is the sampling interval (s); m is the finite number of terms in the unit impulse response model. K_u is a proportional gain [mmHg/(μg/kg/min)]; T_c is a time constant (s); L is dead time (s). The parameters were set at m = 30, ΔT = 10, K_u = 20/3, T_c = 49, and L = 10.

B. AP response emulated by DCNN

1) DCNN structure. The DCNN structure was composed of five convolutional layers followed by two fully connected layers. This structure was determined by trial and error. An image (i.e., pixel values) describing the previous input-output data was applied to the input layer in the DCNN. The input layer was composed of previous NE infusion rates and the

output of AP responses. Input values to DCNN consisted of a nonlinear autoregressive model:

$$\Delta AP'(t) = f(\Delta AP^*(t-1), \ldots, \Delta AP^*(t-8), u(t-1), \ldots, u(t-8)) \quad (3)$$

where $AP'(t)$ is the AP change predicted by DCNN. $\Delta AP^*(t-q)$ is the AP response changed by the NE infusion at a previous sampling point. The amount of previous data for Eq. (3) (i.e., q = 1 to 8) was decided by trial and error, considering the nonlinear dynamic response with dead time. The input values were sent through the convolutional, fully connected, and output layers.

The convolution operation in each layer is described in the following equation:

$$C_i(\boldsymbol{y}) = \max(0, \boldsymbol{w}_i * \boldsymbol{y} + \boldsymbol{b}_i), \quad (4)$$

where $\boldsymbol{y}$ is observed signals, $\boldsymbol{w}_i$ is filter kernels, $\boldsymbol{b}_i$ is biases, and * is the convolution operation. The convolutional layers can learn multiple filter kernels as feature maps. For this study, rectified linear unit was applied as the activation function to the output of convolutional layers. In general, the pooling operation provides a form of translation invariance; however, it was excluded in this study because pixel values of an image input to DCNN strongly corresponded to the time-course data on previous drug infusion rates and AP responses. The final convolution layer is followed by fully connected layers.

2) DCNN Learning. Before AP control, DCNN was trained using ΔAP^* response to random inputs. The infusion rate of NE was randomly assigned between −12 and 12 μg/kg/min. The input and output values were normalized for DCNN learning. The loss function in the learning process was the mean square error between correct and DCNN outputs. The Adam optimization algorithm was used for the learning:

$$\varphi_t = \varphi_{t-1} - \alpha E[g]/\sqrt{E[g^2]}, \quad (5)$$

where φ is the learning parameter; α is the learning rate; g is the gradient; E is the expectation value.

The size of filter kernels was set at 3 × 3, and the feature maps were as follows: 32, 16, 8, 16, and 32 feature maps from the first to final layers, respectively. These optimal values were determined by trial and error. The padding process prevented reduction of the image size by image filtering. In the fully connected layers, the number of elements was set at 8 in each layer. The mini-batch size was 30, the learning rate (α) was 0.001, and the number of epochs was 300.

3) Nonlinear System identification. The result of nonlinear dynamic system identification (i.e., learning of SNN or DCNN) directly links to a control performance. Here, the SNN structure (i.e., two fully connected layers) was consistent with that of DCNN without the convolutional layers; the parameters for SNN were the same as those of DCNN. The drug infusion rates of NE as the system input were pseudo-randomly disturbed between 0 and 10 μg/kg/min. The learning curves for SNN and DCNN were obtained from the training and test data. The accuracy of DCNN after learning was compared with that of SNN by using the same test data.

Nonlinear system identification was performed by using the input (i.e., infusion rates) and output (i.e., AP responses) data. Fig. 1 shows the learning curves and the predicted outputs in SNN and DCNN. The learning process in SNN and DCNN was completed around 100 and 20 epochs, respectively. The output values predicted by DCNN were closely consistent with those of SNN, and they sufficiently mimicked actual AP responses (mean absolute errors ± S.D.: 4.97 ± 2.56 and 4.23 ± 2.95 mmHg in SNN and DCNN, respectively).

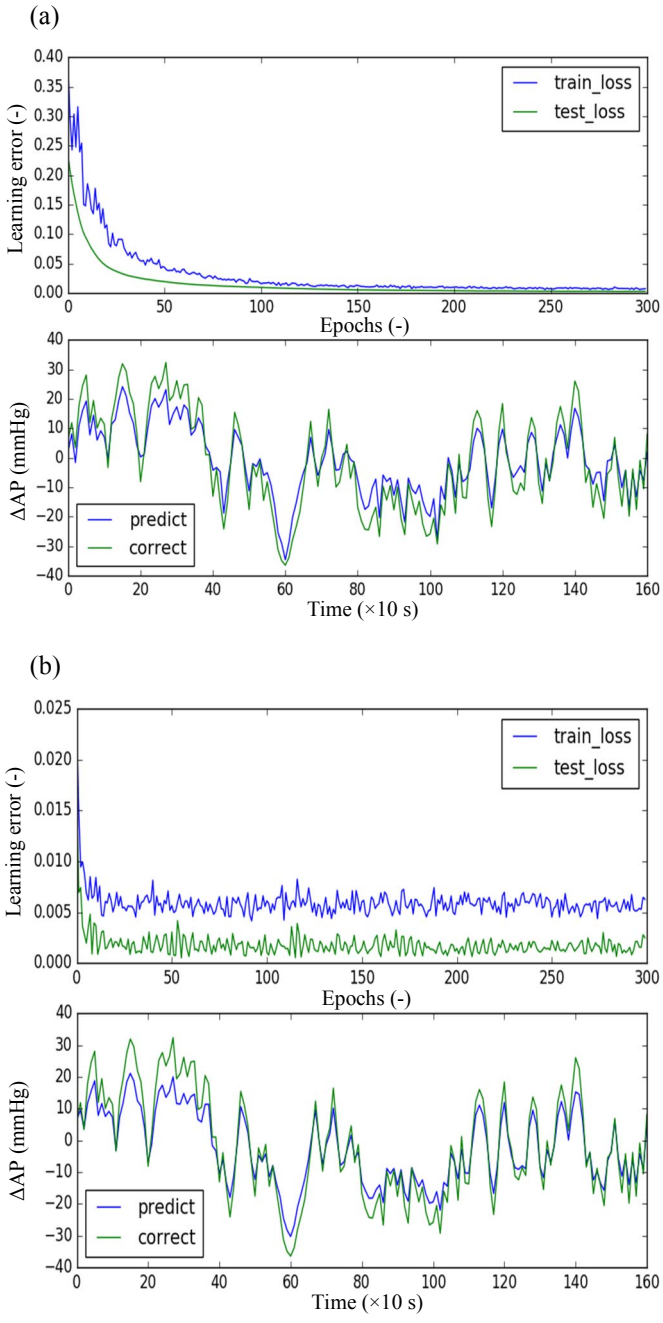

Fig. 1. The learning curves (*upper*) and the predicted outputs (*lower*) after the nonlinear system identification of (a) SNN and (b) DCNN.

C. DCNN controller

(1) *Block diagram for AP control*. Fig. 2 shows a block diagram of the DCNN-based designed controller. During AP control, DCNN recursively learned the feature of the AP response to a NE infusion every 10 s (i.e., each sampling point): the stochastic gradient descent (SGD) optimization algorithm with the leaning rate of 0.03. The sufficiently learned DCNN was used to forecast future ΔAP^* responses. The initial weights of DCNN were acquired from the offline learning results.

(2) *Cost function*. The objective of the AP control was to decide the optimal infusion rate of NE to minimize the following cost function:

$$Q(t) = \sum_{p=0}^{n} |d(t+p) - \Delta AP'(t+p)|, \qquad (6)$$

where n is a prediction horizon, and its optimal value was set at 4. The future output value of $\Delta AP'(t+p)$ was predicted by DCNN; $d(t+p)$ is a target value; $\Delta AP'(t+p)$ is the AP output estimated by a DCNN controller. The cost function $Q(t)$ was minimized by the Nelder−Mead simplex method [13].

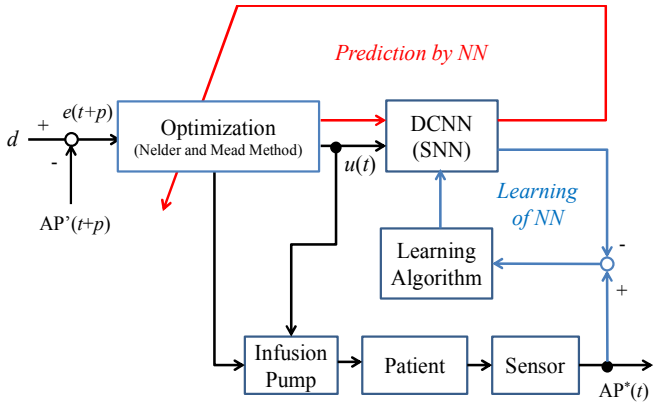

Fig. 2. The block diagram for AP control: $u(t)$ is infusion rate of NE; d is a desired value; $e(t+p)$ is error between the desired value and AP response by DCNN; $AP^*(t)$ is actual AP response at the present time; $AP'(t+p)$ is AP responses predicted by DCNN. *Red* lines: the predicted loop by ANN; *blule* lines: the learning loop for ANN.

III. AP Control by DCNN Controller

A. Evaluation Methods

The adaptive predictive controllers for this study were based on SNN (i.e., no convolutional layers) and DCNN. The total time for AP control was set for 4,000 s. Each controller updated the infusion rate of NE every 10 s, in accordance with the sampling rate of 0.1 Hz. The NE infusion rate was limited between 0 and 10 μg/kg/min. Every sampling point, the desired value for AP control was first set at +20 mmHg, and it was then changed to +30 mmHg (*dotted* lines in Figs. 3 to 6). These controllers were also evaluated under the unknown AP response [the half sensitivity in Eq. (1)] to a drug.

B. Simulation Results

Figs. 3 and 4 represent the simulation results of SNN and DCNN controllers, respectively. Regardless of sufficient learning (i.e., correct results of nonlinear dynamic system identification) before online control, the SNN controller had the hunting of AP output especially during the period between 3,000 and 4,000 s (Fig. 3). Namely, the hunting of the calculated input values reflected the variated AP response because of insufficient online learning.

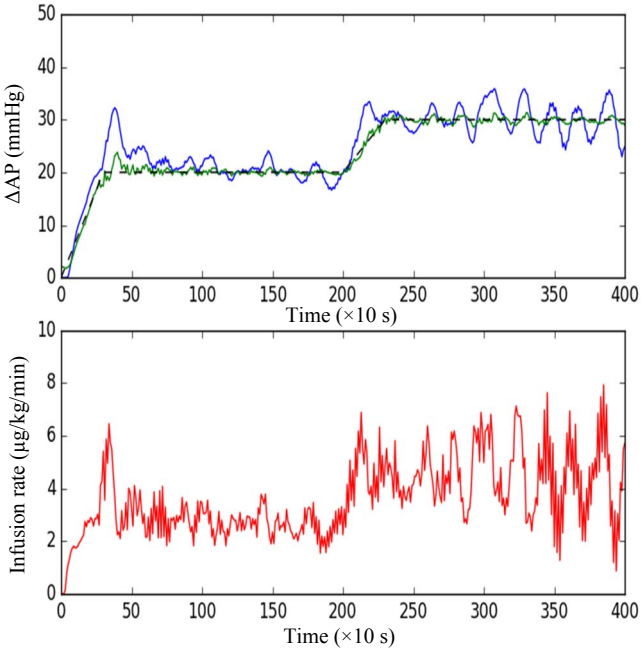

Fig. 3. Simulation results of AP control by using a SNN controller: AP response (*upper*) and the infusion rate of NE (*lower*). *Blue* line, actual AP response; *green* line, SNN response; *dotted* line, desired values; *red* line, drug infusion rate.

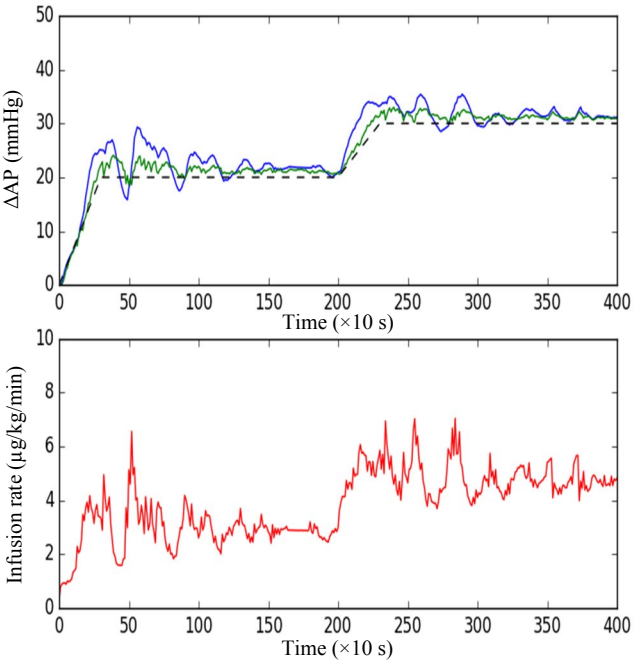

Fig. 4. Simulation results of AP control by using a DCNN controller: AP response (*upper*) and the infusion rate of NE (*lower*). *Blue* line, actual AP response; *green* line, DCNN response; *dotted* line, desired values; *red* line, drug infusion rate.

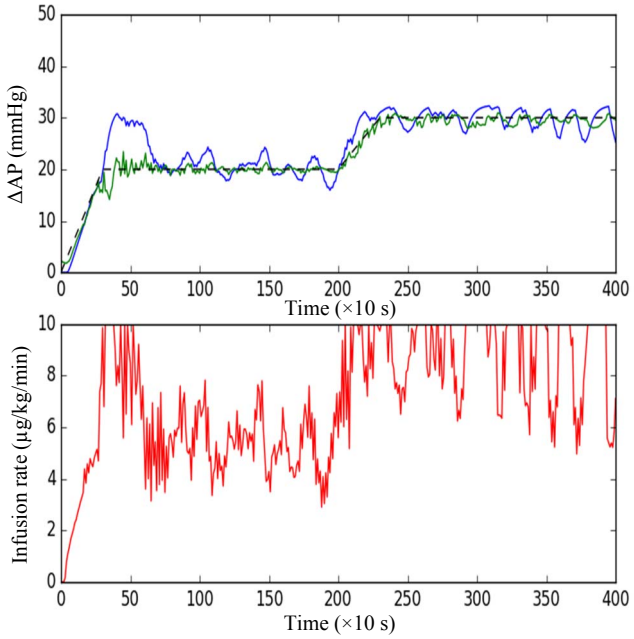

Fig. 5. Simulation results of AP control by a SNN controller: AP response with half sensitivity to a drug (*upper*) and the infusion rate of NE (*lower*). *Blue*, actual AP response; *green*, SNN response; *dotted*, desired values; *red*, drug infusion rate.

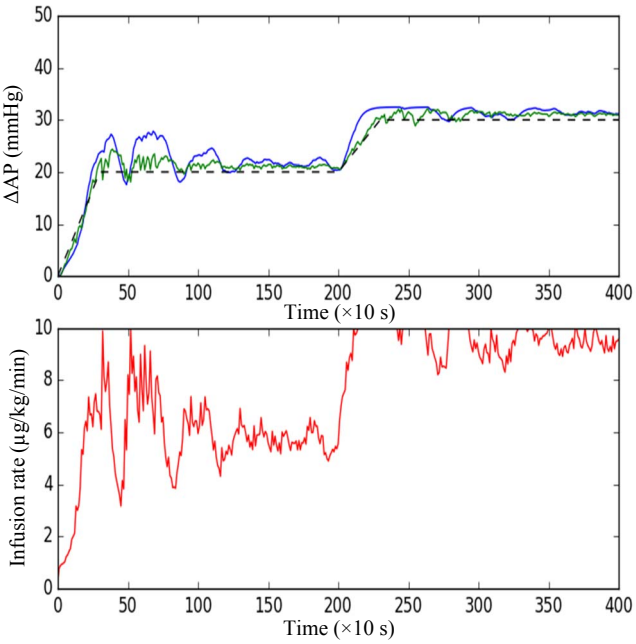

Fig. 6. Simulation results of AP control by a DCNN controller: AP response with half sensitivity to a drug (*upper*) and the infusion rate of NE (*lower*). *Blue*, actual AP response; *green*, DCNN response; *dotted*, desired values; *red*, drug infusion rate.

In contrast, the AP output regulated by the DCNN controller converged to the desired values (i.e., +20 and +30 mmHg) (Fig. 4) without hunting, compared to the result of the SNN controller. The mean absolute errors (± S.D.) between the desired and actual AP responses were 2.33 ± 2.05 and 2.57 ± 1.99 mmHg in the SNN and DCNN controllers, respectively. The mean absolute errors (± S.D.) between the online learning results of SNN and DCNN controllers and actual AP responses were 2.19 ± 1.86 and 1.54 ± 1.43 mmHg, respectively, which reflected the prediction accuracy of future outputs.

Figs. 5 and 6 show the simulation results of SNN and DCNN controllers under the unknown condition (i.e., half sensitivity to drug infusion). The SNN and DCNN controllers completed a stable control, regardless of the unknown AP response. The hunting of AP output in the SNN controller was prevented because of the input limitation of the drug infusion rate (i.e., 10 μg/kg/min). By contrast, the DCNN controller regulated the AP response and barely used the input limitation, especially for the first target value (i.e., +20 mmHg between 0 and 2,000 s). The mean absolute errors (± S.D.) between desired and actual AP outputs were 2.15 ± 2.20 and 2.26 ± 1.68 mmHg in the SNN and DCNN controllers, respectively. The mean absolute errors between the actual and ANN responses were 2.20 ± 2.29 and 1.37 ± 1.33 in the SNN and DCNN controllers, respectively.

IV. Discussion

The accuracy of nonlinear dynamic system identification by ANN links directly to the performance of a designed controller, and DCNN and SNN were able to accurately identify nonlinear responses of a dynamic system. The adequately learned ANN controllers showed the good performance for AP regulation by NE infusion, although the conditions were limited for this study. However, the SNN controller caused hunting in inputs and outputs, regardless of offline learning for a nonlinear dynamic system. To prevent a sudden, significant input change, which may result in the hunting of response data, the cost function to determine the next infusion rate could include an input weight.

Different learning methods for ANN were used in the online (i.e., SGD) and offline (i.e., Adam) periods. The Adam method is effective for mini-batch offline learning; however, this study applied the SGD method to online learning by using a few data in each sampling point, to quickly and flexibly emulate actual AP responses in real time. The SGD method was suitable for DCNN online learning, compared with the Adam method. However, SNN online learning had a poor tracking result of actual AP responses. Therefore, the hyperparameters for ANN controllers should be optimally set to realize a robust and stable control system, considering various learning algorithms.

The features of pharmacological responses will differ among patients and vary with time due to changes in a patient [10],[11]. Moreover, multiple drug infusions will be used for hemodynamic regulation during medical treatments (e.g., hypertension and myocardial infarction). The hemodynamic control system based on ANN will have the ability to efficiently adjust various pharmacological responses among individuals to desired values in real time. Notably, the DCNN controller designed for this study could be extended to a multiple drug infusion system because a substantial number of input and output data can be treated simply as image features; deep layers of DCNN could mimic complicated and interactive responses to multiple drug infusions. Under such situations,

hybrid control systems with artificial intelligence [11] may also be required to use their strengths.

This study used a simple mathematical model of AP response to a NE infusion, although complicated models have been used for previous drug infusion systems of AP control [14]. The flexibility of ANN can be fit to an adaptive predictive control system for nonlinear dynamic response, even for unknown responses or sudden disturbances [10]. Because DCNN has the possibility of automatically emulating a complex model for pharmacological response, it will be an ideal technique for designing automated drug infusion systems for patients.

V. Conclusion

The techniques for SNN and DCNN were applied to the AP control by using a NE infusion, and they resulted in good control performances, even for unknown AP responses. Of note, the designed DCNN controller showed an ability to carry out a more stable AP control than the SNN controller. Because the DCNN-based adaptive predictive controller can accurately determine future AP responses, it will become an efficient tool to construct automated drug infusion systems for hemodynamic regulation. However, further studies for a DCNN controller will be needed under a variety of clinical situations (e.g., a sudden change in a patient's condition), to evaluate robustness and flexibility. Because multiple drugs are commonly used in clinical practice, a DCNN-based multivariate control should be assessed as the next objective of automated drug infusion systems. Even under such control conditions, DCNN could be simply extended to a multivariate control system.

Acknowledgment

This study was partially funded by the Grant–in–Aid for Scientific Research (C) program of the Japan Society for the Promotion of Science (KAKENHI, 25330171; 17K01297).

References

[1] S. I. Rajfer and L. I. Goldberg (1984) Sympathomimetic amines. In: Principles and Practice of Acute Cardiac Care, edited by G. Das and S. Dipankar. Chicago: Year Book Medical, 126–133

[2] R. C. Tarazi (1974) Sympathomimetic agents in the treatment of shock. Ann. Intern. Med. 81:364–371

[3] M.Kaur, M. Pawar, J. K. Kohli, and S. Mishra (2008) Critical events in intensive care unit. Indian journal of critical care medicine: peer-reviewed, official publication of Indian Society of Critical Care Medicine, 12(1) :28–31

[4] M. L. Quinn, N. T. Smith, J. E. Mandel, J. F. Martin, and A. M. Schneider (1988) Automatic control of arterial pressure in the operating room: Safety during episodes of artifact and hypotension? Anesthesiology 68:A327

[5] L. C. Sheppard (1980) Computer control of the infusion of vasoactive drugs. Ann. Biomed. Eng. 8:431–444

[6] C. T. Chen, W. L. Lin, T. S. Kuo, and C. Y. Wang (1997) Adaptive control of arterial blood pressure with a learning controller based on multilayer neural networks. IEEE Trans. Biomed. Eng. 44:601–609

[7] E. A. Woodruff, J. F. Martin, and M. Omens (1997) A model for the design and evaluation of algorithms for closed-loop cardiovascular therapy. IEEE Trans. Biomed. Eng. 44:694–705

[8] G. A. Pajunen, M. Steinmetz, and R. Shankar (1990) Model reference adaptive control with constraints for postoperative blood pressure management. IEEE Trans. Biomed. Eng. 37:679–687

[9] K. S. Stern, H. J. Chizeck, B. K. Walker, P. S. Krishnaprasad, P. J. Dauchot, and P. G. Katona (1985) The self-tuning controller: Comparison with human performance in the control of arterial pressure. Ann. Biomed. Eng. 13:341–357

[10] K. Kashihara, T. Kawada, K. Uemura, et al. (2004) Adaptive predictive control of arterial blood pressure based on a neural network during acute hypotension. Ann. Biomed. Eng. 32:1365–1383

[11] K. Kashihara (2006) Automatic regulation of hemodynamic variables in acute heart failure by a multiple adaptive predictive controller based on neural networks. Ann. Biomed. Eng. 34:1846–1869

[12] K. Kashihara (2016) Deep convolutional neural networks improve vein image quality, Proc. of 17th IEEE International Symposium on Computational Intelligence and Informatics (CINTI 2016), 209–212

[13] J. A. Nelder and R. Mead (1965) A Simplex method for function minimization. Comput. J. 7:308–313

[14] E. A. Woodruff, J. F. Martin, and M. Omens (1997) A model for the design and evaluation of algorithms for closed-loop cardiovascular therapy. IEEE Trans. Biomed. Eng. 44:694–705